

Combined Pressure and Electrical-Resistivity Measurements of Warm Dense Aluminum and Titanium Plasmas

P. Renaudin,* C. Blancard, G. Faussurier, and P. Noiret

Département de Physique Théorique et Appliquée, CEA/DAM Ile-de-France, BP12, 91680 Bruyères-le-Châtel Cedex, France

(Received 29 January 2002; published 7 May 2002)

Electrical resistivity, pressure, and internal energy variation of warm dense correlated titanium (density 0.2 g/cm^3) and aluminum (density 0.1 g/cm^3) plasmas are measured using a homogeneous and thermally equilibrated media produced inside an isochoric closed-vessel plasma. These data are compared to detailed calculations based on the density functional theory. In the studied temperature range ($15\,000\text{--}30\,000 \text{ K}$), it appears that both exchange-correlation and ion-ion interaction treatments are of great importance to calculate accurate theoretical values.

DOI: 10.1103/PhysRevLett.88.215001

PACS numbers: 52.25.Fi, 52.25.Kn, 52.27.Gr

For most materials under many conditions, the equation of state (EOS) and transport coefficients are fairly well known. In strongly coupled plasmas (SCP's) characterized by Coulomb potential energy between plasma particles greater than their average kinetic energy, the physics is quite complicated due to the strong interaction of individual particles with each other [1]. The knowledge of the transport and thermodynamic properties of such plasmas is one of the key points in high-pressure electrical discharges, inertial confinement fusion, astrophysics, and dusty plasmas research [2]. At the present stage, there are few theories that can produce thermodynamic data, transport coefficients, and optical properties of partially ionized plasmas in a self-consistent way [3]. Because of the difficulty to perform accurate measurements of these quantities in SCP's, the theory is the main source of information and remains untested in most of the cases [4–6]. Some experiments have been done to measure the electrical resistivity [7–9] or the optical reflectivity [10,11] of SCP's. However, no experimental EOS investigations have been performed in the thermodynamic regime of SCP's.

In this Letter, we report on the first combined electrical-resistivity, pressure, and internal energy variation measurements of well-known mass density plasmas. Two elements have been considered: a simple metal (aluminum) and a transition metal (titanium), which present a complex electronic structure and provide a well-known challenge for theoretical modeling.

The experiments were performed in an isochoric closed-vessel plasma (EPI), where a sample goes from the metallic solid state at normal density and room temperature to a well-known density plasma regime, through liquid and vapor phases. EPI combines two techniques: a high-pulse power bank to obtain a fast heating of the metallic sample and a high-pressure closed vessel. A schematic diagram of the experimental setup is shown in Fig. 1. The body of the vessel consists of an alternate stack of autofretted bimetallic rings (1 cm thickness) and electrical insulator Kapton foils ($125 \mu\text{m}$). Actually, the maximal pressure obtainable (1.5 GPa) is limited by the applied axial clamp-

ing force and the sliding friction coefficient of the Kapton foil. During the final mounting of the vessel, this axial force is set to 120 to 150 tons. A sapphire ring is bound in the center of each high-pressure ring forming (one stacked) a tube of 20 cm in length and 1.2 cm in diameter. Sapphire is a good thermal insulator. It sustains high pressure very well and is transparent in the spectral range $0.2\text{--}5 \mu\text{m}$. The external surface of the sapphire is coated with aluminum to confine the plasma radiation by a mirror reflection. A maximal temperature of $40\,000 \text{ K}$ is fixed to limit the sapphire damages and plasma pollution due to the wall ablation. A $25\text{-}\mu\text{m}$ -thick pure titanium or aluminum foil at normal density and room temperature is placed inside the vessel with a shape that fills the internal volume. This foil is in contact at both ends with two electrodes, of the same metal as the foil, held in two locking parts. We use a slow capacitor bank charged to an energy of 225 kJ to produce a current, which rises to a peak of 80 to 100 kA in $150 \mu\text{s}$. Current is driven from four capacitors connected in parallel, totaling 2.42 mF, and is switched by

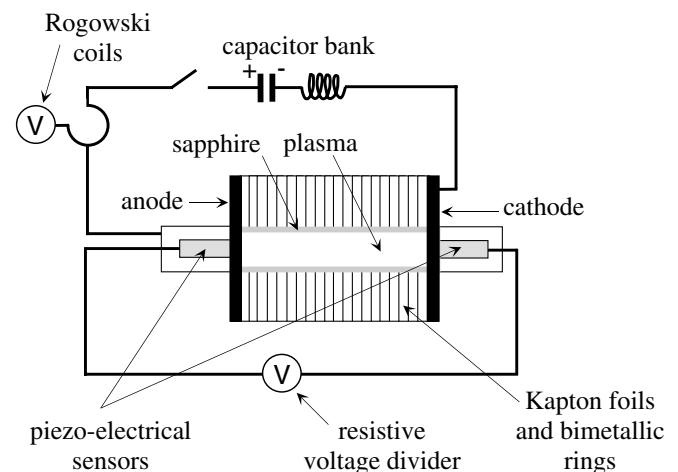


FIG. 1. Experimental setup of the EPI device. A pulse power bank produces a current which passes from the electrodes to the foil. The plasma expansion is tamped by sapphires.

a pressurized spark gap switch. Internal inductance of the circuit without the foil is $6 \mu\text{H}$, which is large compared to the inductance of the foil ($0.4 \mu\text{H}$). With this experimental setup, the sample is heated in a hundred of microseconds. The plasma volume is controlled mechanically by the closed-vessel walls. The characteristic time of the pulse-power supply is long enough to allow the formation of a homogeneous plasma, and is short enough to limit the effects of the wall ablation. The assumption of homogeneity is supported by different theoretical reasons: (i) The duration of energy input is about $100 \mu\text{s}$ and the sound-propagation time across a 0.6-cm -thick ionized vapor of aluminum or titanium is about $4 \mu\text{s}$, according to the LANL SESAME EOS [12]. (ii) The diameter of a $10\,000 \text{ K}$ temperature free-burning arc at equilibrium dissipating the same power as in our experiment is 2.5 cm , which is twice the inner diameter of the vessel. (iii) The skin depth in a conductor having the same resistivity as the plasma, at a frequency of 5 kHz (bandwidth derived from a Fourier analysis of the current signal), is 6 times as large as the inner radius of the vessel. (iv) The magnetic pressure for a 100 kA current in a 1.2-cm -diameter cross section is about 30 MPa , which is small compared to the 1 GPa measured in the vessel during the experiment. Since the plasma is homogeneous, the density depends only on the initial mass of the material placed in the vessel (a mass of 2.2 g leads to a homogeneous density of 0.1 g/cm^3). In one electrical discharge, the experimental setup allows simultaneous measurements of EOS data (internal energy variation, pressure, and density) and electrical resistivity along an isochore. A Rogowski belt surrounds one electrode to measure the time derivative of the current, and a resistive divider is used to measure the voltage drop across the plasma. The time derivative dI/dT of the current and the inductance L of the plasma ($0.4 \mu\text{H}$) are small enough to make the $L \times dI/dT$ term negligible compared to the measured voltage. Therefore, no inductive correction is needed to obtain the plasma resistivity from the current and voltage measurements, except at the very beginning of the discharge. Two calibrated piezoelectrical sensors were used to measure the pressure during the discharge. There is no contact between them and the plasma. A small piston is placed between each looking part at the ends of the sapphire tube, and transmits the pressure to the sensor.

The electrical resistance, the pressure, and the variation of internal energy measured during a titanium experiment are plotted as a function of time on Fig. 2. After the rapid liquefaction of the foil, the vaporization occurs at the end of the phase labeled (1) in Fig. 2. During the evaporation, a nonequilibrium multiphase system is obtained: the liquid and the vapor are heated independently. A short delayed ionization of the first bubbles of vapor can be seen during the phase labeled (2). At point (3) (at time $130 \mu\text{s}$), the effective phase of vaporization begins. At that time, conductivity and pressure rise quickly. The heating becomes isochoric at time (4) when the vapor ionization induces an

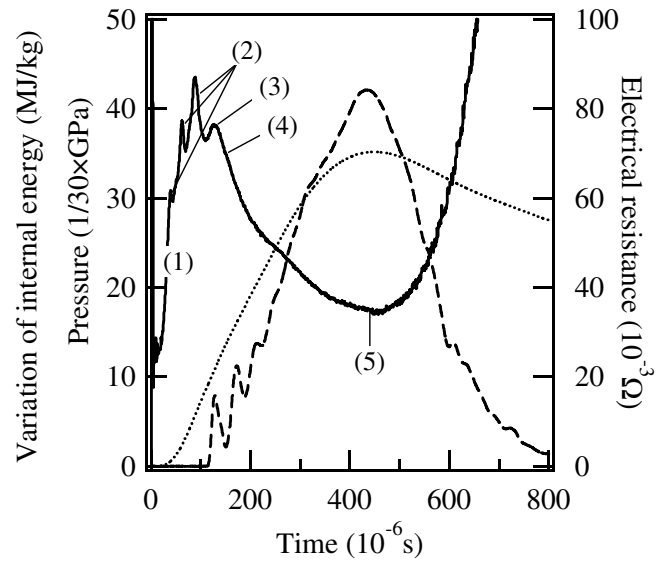


FIG. 2. Measurements of the internal energy variation (dotted line), electrical resistance (solid line), and pressure (dashed line) of the titanium plasma as a function of time.

arc regime. At the point (5) (at time $420 \mu\text{s}$), maximums of electrical conductivity and pressure are reached. Beyond point (5), cooling begins. Finally, the interpretation of the resistance $R(t)$ in term of resistivity $\rho(t)$ is meaningful only at times when the plasma is homogeneous, i.e., between points (4) and (5). At each shot, the energy input and the electrical resistivity of the plasma are inferred from the current and voltage measurements. The resistivity of the plasma is determined by using the relation $\rho(t) = \pi r^2(t)R(t)/l(t)$, where the length $l(t)$ and the radius $r(t)$ of the plasma are the length and the radius of the vessel, respectively. The uncertainty in the current and voltage measurements produces a 15% uncertainty in the resistance of the plasma. The internal energy variation ΔU_{int} can be evaluated from the electrical energy input E_{el} and is given by $\Delta U_{\text{int}} = (E_{\text{el}} - E_{\text{rad}}) + \Delta W$, where E_{rad} are the thermal losses at the vessel walls. The mechanical work loss ΔW due to the vessel expansion under pressure is less than 1% of E_{el} and can be neglected. The thermal losses are assumed to be radiative during the plasma phase, and negligible before. The internal energy is obtained at each time by resolving the following differential equation: $dU_{\text{int}}/dt = dE_{\text{el}}/dt - \alpha \sigma_0 S T (U_{\text{int}})^4$, where σ_0 is the Stefan-Boltzmann constant, S is the plasma surface, and T is written as a function of U_{int} by using SESAME tables [12]. Because of the isochoric and monophasic assumption, $dU_{\text{int}}/dt = 0$ at point (5), where maximums of electrical conductivity and pressure are reached. At that time, α is measured and depends only on the instantaneous power dE_{el}/dt .

We have also developed a model (SCAALP) based on the density functional theory for hot dense plasmas, where electronic structure and ionic distribution are determined self-consistently. The plasma is considered as an effective

classical system of virtual neutral particles [neutral pseudoatom (NPA)] interacting via an interatomic effective potential, ϕ . Electrons of the NPA satisfy a Schrödinger equation with an effective central symmetric potential V_{eff} . Both ϕ and V_{eff} are determined by the electronic structure and the ionic distribution of the plasma. They naturally appear while looking for the best unperturbed one-electron Hamiltonian with the Gibbs-Bogolyubov inequality (GBI) [13]. It is assumed that the adiabatic approximation (Born-Oppenheimer approximation) is valid and that two electrons are independent of each other when one electron is in a NPA and the other one is in another NPA (no molecular nor cluster formations are allowed). We went beyond Ref. [14] by taking into account the polarization and the correlation effects of the continuum electrons, as well as a part of the exchange interaction within the interatomic effective potential. Two exchange-correlation functionals have been considered. The first one, proposed by Vosko *et al.* (VWN) is well suited for solid state physics [15]. The second one, proposed by Perrot and Dharma-wardana (PD), is more adapted for plasma physics and is consistent with VWN at zero temperature [16]. We look for the best reference system using the GBI [13,17] to obtain the radial distribution function of the ionic subsystem from ϕ . In this paper, we have considered only the one-component plasma as a reference system. This method gives us (i) access to the excess free energy of the ionic subsystem that is not reachable by simply using the hypernetted chain equations, (ii) ensures a complete thermodynamical consistency of our model, and (iii) makes possible the evaluation of various ionic transport coefficients. Electrical resistivity is obtained using the Ziman formula [18,19] and electronic pressure is calculated following Blenski and Ishikawa [20].

The electrical resistivity is plotted as a function of the temperature (deduced from the SESAME tables for experimental data) in Fig. 3 for aluminum and in Fig. 4 for titanium. The vertical error bars indicate the uncertainty in the resistivity measurement. The temperature uncertainty is assumed to be equal to the electrical energy uncertainty, i.e., 15%. Concerning aluminum, an experimental measurement from [9] has been added in Fig. 3. Other experimental results obtained from [7,8] are in rather good agreement with our data at low temperature and are not shown. SCAALP results obtained from the exchange-correlation VWN and the PD functionals are plotted in Fig. 3. Other calculations performed by Perrot and Dharma-wardana, labeled PDW [21], are also shown. The PDW model uses the exchange-correlation functional implemented into SCAALP-PD but differs by the treatment of the ionic structure. At high temperature, the three models give very similar results that are consistent with the experimental value. This indicates that both the exchange-correlation and the ion-ion interaction treatments have here a minor influence on theoretical results. PDW

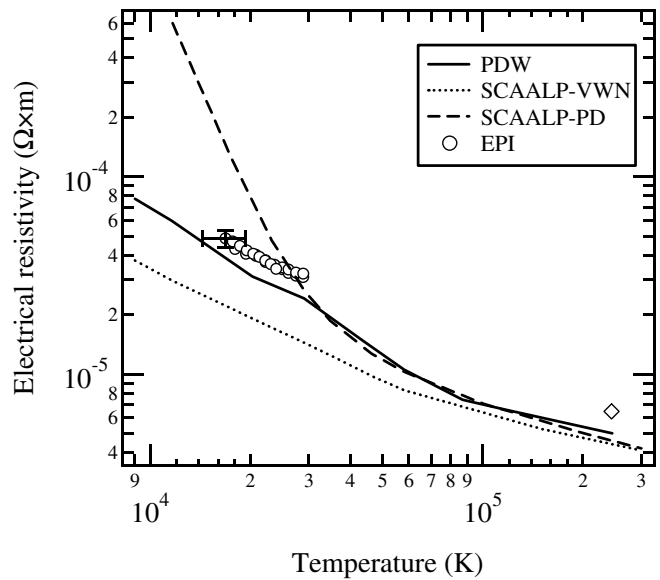


FIG. 3. Electrical resistivity of aluminum at a density of 0.1 g/cm^3 as a function of temperature. Theoretical results from SCAALP with two different exchange-correlation functionals and from Ref. [21] labeled PDW are also shown. The \diamond represents one experimental datum from Ref. [9].

and SCAALP-PD models agree well in the temperature range $30\,000\text{--}300\,000 \text{ K}$, whereas SCAALP-VWN predicts lower resistivities for decreasing temperature, showing the influence of the exchange-correlation treatment, as recently put forward by Suhr, Barbee, and Yang [22]. For lower temperatures, PDW, SCAALP-PD, and SCAALP-VWN disagree. This illustrates the competitive influence of the ion-ion interaction and the exchange-correlation treatments on the theoretical results. Concerning titanium (see Fig. 4), our experimental data are compared to SCAALP calculations. Once again, the influence of the exchange-correlation treatment is clearly shown. For temperatures greater than $15\,000 \text{ K}$, SCAALP-VWN underestimates by a factor of 4 the experimental data, whereas the SCAALP-PD calculations

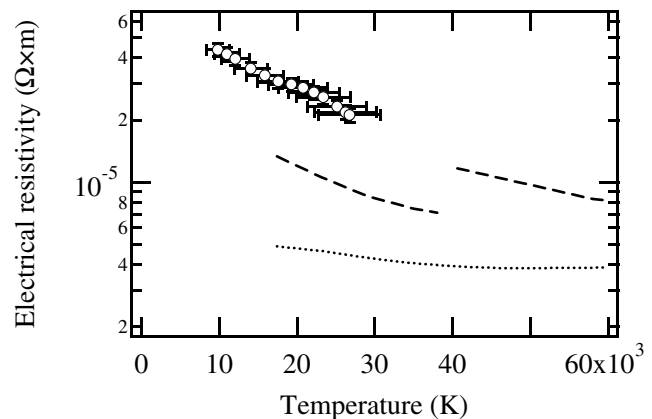


FIG. 4. Same as Fig. 3 for titanium at a density of 0.2 g/cm^3 .

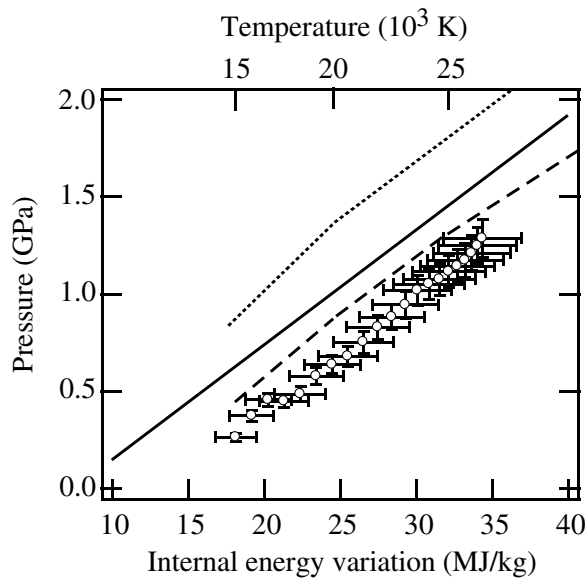


FIG. 5. Pressure of titanium at a density of 0.2 g/cm^3 as a function of internal energy variation. The \circ 's are the measured data. The solid line is the pressure calculated by SESAME, where the reference energy is the internal energy at solid density and room temperature. The dashed and dotted lines are the pressure calculated by SCAALP-PD and SCAALP-VWN, respectively.

are only 2 times lower. At about 40 000 K, the apparent discontinuity of the SCAALP-PD resistivity is due to the pressure ionization of the significantly occupied $4p$ orbital (typically 0.5 electrons). This process induces a huge change in the scattering state number and, consequently, causes the edge of the electrical resistivity.

The pressure of titanium as a function of internal energy variation is plotted in Fig. 5. We observe that the experimental pressure is lower than the SESAME pressure. It can be noticed that our experimental data cover the interpolation area of the SESAME EOS, where mismatches between adjacent theories exist. The pressures calculated by SCAALP are plotted as a function of temperature. They differ from each other by 25% to 40% in the studied temperature range and are less sensible to the exchange-correlation treatment than electrical resistivity. SCAALP-PD pressure is lower than SESAME pressure at a given temperature and is closer to our experimental data.

To summarize, we have carried out an experiment measuring directly electrical resistivity, pressure, mass density, and internal energy variation of strongly coupled aluminum and titanium plasmas in the density and temperature ranges ($0.1\text{--}0.2 \text{ g/cm}^3$; $15\,000\text{--}30\,000 \text{ K}$). Our experimental results are in agreement with the theoretical model based on the density functional theory, and show

that exchange correlation and ion-ion interaction treatments have a strong impact on theoretical results in the studied thermodynamic regime.

The authors thank J.F. Benage and M.S. Murillo for providing their experimental data and F. Perrot and M. W. C. Dharma-wardana for providing their theoretical results. We also thank S. Kiyokawa for useful discussions and B. Loffredo and M. Sonnaert for their technical assistance during the course of this work.

*Electronic address: patrick.renaudin@cea.fr

- [1] S. Ichimaru, in *Statistical Plasma Physics, Vol. II: Condensed Plasmas*, Frontiers in Physics Vols. **87–88** (Addison-Wesley, New York, 1994).
- [2] Good reviews are found in the special issue of *Contrib. Plasma Phys.* **41** (2001).
- [3] F. Perrot and M. W. C. Dharma-wardana, *Phys. Rev. E* **52**, 5352 (1995); J. Chihara, Y. Ueshima, and S. Kiyokawa, *Phys. Rev. E* **60**, 3262 (1999).
- [4] G. A. Rinker, *Phys. Rev. B* **31**, 4207 (1985); *Phys. Rev. A* **37**, 1284 (1988).
- [5] Y. T. Lee and R. M. More, *Phys. Fluids* **27**, 1273 (1984).
- [6] R. Redmer, *Phys. Rev. E* **59**, 1073 (1999).
- [7] A. W. DeSilva and J. D. Katsourous, *Phys. Rev. E* **57**, 5945 (1998).
- [8] I. Krisch and H. J. Kunze, *Phys. Rev. E* **58**, 6557 (1998).
- [9] J. F. Benage, W. R. Shanahan, and M. S. Murillo, *Phys. Rev. Lett.* **83**, 2953 (1999).
- [10] A. Ng *et al.*, *Phys. Rev. Lett.* **72**, 3351 (1994).
- [11] A. N. Mostovych and Y. Chan, *Phys. Rev. Lett.* **79**, 5094 (1997).
- [12] SESAME: The Los Alamos National Laboratory Equation of State Database, Report No. LA-UR-92-3407, edited by S. P. Lyon and J. Johnson, Group T-1.
- [13] R. P. Feynman, *Statistical Mechanics: A Set of Lectures* (Addison-Wesley, New York, 1972).
- [14] S. Kiyokawa, *J. Phys. Soc. Jpn.* **64**, 4708 (1995).
- [15] S. H. Vosko, L. Wilk, and M. Nusair, *Can. J. Phys.* **58**, 1200 (1980).
- [16] F. Perrot and M. W. C. Dharma-wardana, *Phys. Rev. A* **30**, 2619 (1984).
- [17] J. P. Hansen and I. R. McDonald, *Theory of Simple Liquids* (Academic, New York, 1986), 2nd ed.; F. J. Rogers *et al.*, *Phys. Rev. A* **28**, 2990 (1983).
- [18] J. M. Ziman, *Principle of Theory of Solids* (Cambridge University Press, Cambridge, 1972).
- [19] H. Minoo, C. Deutsh, and J. P. Hansen, *Phys. Rev. A* **14**, 840 (1976).
- [20] T. Blenski and K. Ishikawa, *Phys. Rev. E* **51**, 4869 (1995).
- [21] F. Perrot and M. W. C. Dharma-wardana, *Phys. Rev. A* **36**, 238 (1987).
- [22] M. P. Suhr, T. W. Barbee III, and L. H. Yang, *Phys. Rev. Lett.* **86**, 5958 (2001).